

Field-Induced Gaps in the Frustrated Spin Ladder

Nobuhisa OKAZAKI, Kiyomi OKAMOTO¹ and Tôru SAKAI

*Faculty of Science, Himeji Institute of Technology,
Kamigouri-cho, Akou-gun, Hyogo 678-1297, Japan*
¹*Department of Physics, Tokyo Institute of Technology,
Oh-okayama, Meguro-ku, Tokyo 152-0033, Japan*

(Received October 30, 2018)

We study the magnetization process of the $S = 1/2$ antiferromagnetic spin ladder in the presence of the second and the third-neighbor couplings which lead to frustration with the typical nearest-neighbor coupling. We use degenerate perturbation theory and level spectroscopy analysis of the numerical diagonalization data of the Hamiltonian for finite systems. We find two kinds of plateaux at half the saturation moment in the magnetization curve. One is mainly due to the second-neighbor couplings and the other to the third-neighbor couplings. The mechanisms of these two plateaux are quite different with each other.

KEYWORDS: spin ladder, magnetization plateau, frustration

The spin gap is a current topic of interest in strongly correlated electron systems because it is related to various interesting quantum phenomena such as high- T_c superconductivity. Since the Lieb-Schultz-Mattis (LSM) theorem¹⁾ was recently generalized to the magnetization process²⁾, a field-induced spin gap has attracted a great deal of interest in the field of low-dimensional magnets. The extended LSM theorem predicts that a 1D quantum spin system possibly has gaps which are observed as plateaux in the magnetization curve under the condition of quantization of the magnetization, described as

$$Q(S - m) = \text{integer}, \quad (1)$$

where Q is the spatial period of the ground state measured by the unit cell. S and m are the total spin and the magnetization per unit cell, respectively. Applying this theorem to the spin ladder, only the well-known spin gap^{3,4,5)} is expected to appear at $m = 0$, as far as $Q = 1$. Several theoretical analyses, however, predicted that field-induced gaps would also appear at a finite magnetization, with some modifications in the structure of the unit cell such as three-leg⁶⁾ and bond-alternating ladders.⁷⁾

On the other hand, spontaneous breaking of the translational symmetry ($Q \geq 2$) can also yield magnetization plateaux. The previous size scaling study⁸⁾ based on conformal field theory indicated the possibility of the plateau at $m = 1/2$ due to the two-fold degeneracy of the ground state (i.e., $Q = 2$) in the standard spin ladder with the second-neighbor (2-N) interaction J_2 . In the plateau phase, the singlet pair state and the $|\uparrow\uparrow\rangle$ state of the rung are expected to locate alternately along the leg. A similar mechanism of the field-induced gap was predicted for the zigzag ladder equivalent to the bond-alternating chain with the 2-N interaction.^{10,9,11)}

In this paper, we investigate another mechanism of the plateau formation due to the introduction of the third-neighbor (3-N) coupling J_3 . We also present a typical

phase diagram of the J_3 - J_2 plane, obtained by the level spectroscopy method analyzing the finite cluster diagonalization data.

We consider the $S=1/2$ antiferromagnetic spin ladder with 2-N and 3-N exchange interactions in a magnetic field described by the Heisenberg Hamiltonian

$$\hat{H} = \hat{H}_0 + \hat{H}_Z \quad (2)$$

$$\begin{aligned} \hat{H}_0 = & J_1 \sum_i^L (\mathbf{S}_{1,i} \cdot \mathbf{S}_{1,i+1} + \mathbf{S}_{2,i} \cdot \mathbf{S}_{2,i+1}) \\ & + J_\perp \sum_i^L \mathbf{S}_{1,i} \cdot \mathbf{S}_{2,i} \\ & + J_2 \sum_i^L (\mathbf{S}_{1,i} \cdot \mathbf{S}_{2,i+1} + \mathbf{S}_{2,i} \cdot \mathbf{S}_{1,i+1}) \\ & + J_3 \sum_i^L (\mathbf{S}_{1,i} \cdot \mathbf{S}_{1,i+2} + \mathbf{S}_{2,i} \cdot \mathbf{S}_{2,i+2}) \end{aligned} \quad (3)$$

$$\hat{H}_Z = -H \sum_i^L (S_{1,i}^z + S_{2,i}^z), \quad (4)$$

under the periodic boundary condition, where J_1 , J_\perp , J_2 and J_3 denote the coupling constants of the leg, rung and 2-N (diagonal) and 3-N exchange interactions, respectively (Fig. 1). Hereafter we put $J_\perp=1$. \mathcal{H}_Z is the Zeeman term where H denotes the magnetic field along the z -axis and the eigenvalue M of the conserved quantity $\sum_i (S_{1,i}^z + S_{2,i}^z)$ is a good quantum number. The macroscopic magnetization is represented by $m = M/L$.

In order to consider the possibility and the mechanism of the magnetization plateau at $m = 1/2$ we use the degenerate perturbation theory around the strong rung coupling limit $J_1, J_2, J_3 \ll 1$.¹²⁾ We introduce a pseudo spin \mathbf{T} for each rung pair and map the two original states ($|\uparrow\downarrow\rangle - |\downarrow\uparrow\rangle)/\sqrt{2}$ and $|\uparrow\uparrow\rangle$ of the \mathbf{S} picture to the $|\downarrow\rangle$ and $|\uparrow\rangle$ states of \mathbf{T} , neglecting the other two states

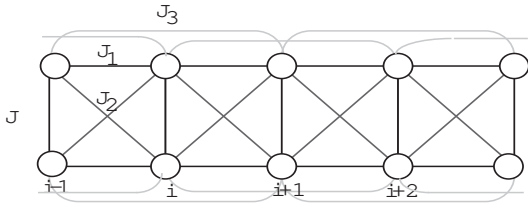


Fig. 1. Spin ladder with 2-N and 3-N exchange interactions along the diagonals.

$(|\uparrow\downarrow\rangle + |\downarrow\uparrow\rangle)/\sqrt{2}$ and $|\downarrow\downarrow\rangle$. After the mapping, we obtain the effective Hamiltonian

$$\begin{aligned} \hat{H}_{\text{eff}} = & (J_1 - J_2) \sum_i^L (T_i^x \cdot T_{i+1}^x + T_i^y \cdot T_{i+1}^y) \\ & + \frac{J_1 + J_2}{2} \sum_i^L (T_i^z \cdot T_{i+1}^z) \\ & + J_3 \sum_i^L (T_i^x \cdot T_{i+2}^x + T_i^y \cdot T_{i+2}^y) \\ & + \frac{J_3}{2} \sum_i^L (T_i^z \cdot T_{i+2}^z). \quad (5) \end{aligned}$$

This effective Hamiltonian describes the $T = 1/2$ XXZ chain with 2-N interactions, where J_2 and J_3 control the XXZ anisotropies and 2-N couplings, respectively, with fixed J_1 . We note that the XXZ anisotropy parameters of the NN and 2-N interactions are different from each other. Well-established works on this model have revealed the following properties:¹³⁾ the system has three phases; the spin fluid (gapless), Néel (gapped) and dimer (gapped) phases. The $J_2 = J_3 = 0$ case is clearly in the gapless phase and sufficiently large J_2 (J_3) yields the Néel (dimer) phase via the Berezinski-Kosterlitz-Thouless (BKT) transition.^{14, 15)} The boundary between the Néel and dimer phases is the Gaussian line. The above properties lead us to the conclusion that J_2 and J_3 give rise to the plateau at $m = 1/2$ in the original system, based on different mechanisms; the Néel state and the dimer state, in the language of pseudo spins. The two plateaux are hereafter called the plateau A (Néel) and plateau B (dimer). Clearly, both plateau phases should be accompanied by the two-fold degeneracy due to the spontaneous breaking of the translational symmetry.

Next, we perform a numerical analysis for the original Hamiltonian (4) to more quantitatively confirm the realization of two plateaux at $m = 1/2$, predicted by the degenerate perturbation theory. The *level spectroscopy*¹³⁾ is a powerful method to determine the BKT boundary, as well as most second-order transitions in 1D quantum systems. In this method, the phase boundaries can be determined from the level crosses between low-lying excitations. This method is free from the most dominant logarithmic size corrections, which make it difficult to determine the BKT boundaries when conventional methods are applied. Hereafter, $E(L, M, k)$ indicates the lowest eigenvalue of the Hamiltonian \hat{H}_0 in the subspace where

the eigenvalue of $\sum_i (S_{1,i}^z + S_{2,i}^z)$ is M and the momentum is k for the system size L . Using the Lanczos algorithm, $E(L, M, k)$ is calculated for $L = 4n$ (≤ 16), to avoid frustration among the 3-N exchange interactions under the periodic boundary condition. Before investigating the full Hamiltonian, let us briefly demonstrate the powerfulness of level spectroscopy by drawing a phase diagram for the $J_3 = 0$ case, which has already been obtained by conventional methods.⁸⁾ In level spectroscopy, we use the following two excitations given by

$$\begin{aligned} \Delta_1 = & \frac{1}{2} \left\{ E\left(L, \frac{L}{2} + 1, \pi\right) + E\left(L, \frac{L}{2} - 1, \pi\right) \right\} \\ & - E\left(L, \frac{L}{2}, 0\right), \quad (6) \end{aligned}$$

and

$$\Delta_0 = E\left(L, \frac{L}{2}, \pi\right) - E\left(L, \frac{L}{2}, 0\right). \quad (7)$$

When the parameters are swept, the state is gapless or gapped (i.e., plateau) according to whether $\Delta_1 < \Delta_0$ or $\Delta_1 > \Delta_0$, as explained by Okamoto et al.¹⁶⁾ The phase diagram of the J_2 - J_1 plane, obtained by this procedure is shown in Fig. 2. The estimated error bars of the

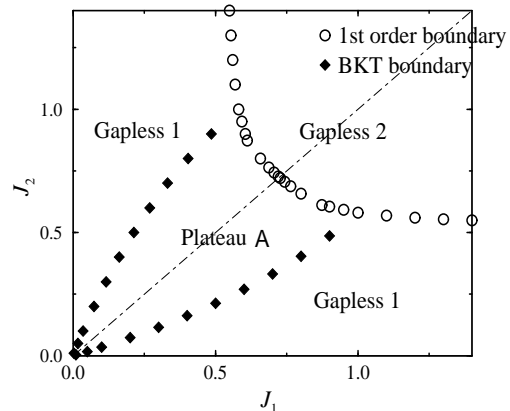


Fig. 2. Phase diagram on the J_2 - J_1 plane at $m = 1/2$.

boundary points are much smaller than the size of the marks. In this phase diagram, in addition to the original spin fluid (gapless 1) phase, there appears another gapless phase (gapless 2). Here we do not touch the gapless 2 phase (equivalent to the $S = 1$ chain at $m = 1/2$; see refs. 8 and 17 for details). Using the effective Hamiltonian eq. (5), we see that the slope of the boundary line between the plateau A and gapless 1 phases is $1/3$ in the limit of $J_1 \rightarrow 0$ (note that H_{eff} of eq. (5) is exact in this limit), as noted by Mila.¹²⁾ In our numerical calculation, we obtain $J_2/J_1 = 0.3350$ when $J_1 = 0.01$, which agrees very well with the exact value $1/3$. This shows the high reliability of our level spectroscopy method. When conventional methods are applied to this problem,^{17, 8)} the slope value in the $J_1 \rightarrow 0$ limit is estimated as $J_2/J_1 \simeq 0.45$, which is much larger than the exact value $1/3$. The reason for this difference is discussed by Okamoto¹⁸⁾ in detail and will be published elsewhere.

Here we consider the full Hamiltonian problem $J_3 \neq 0$.

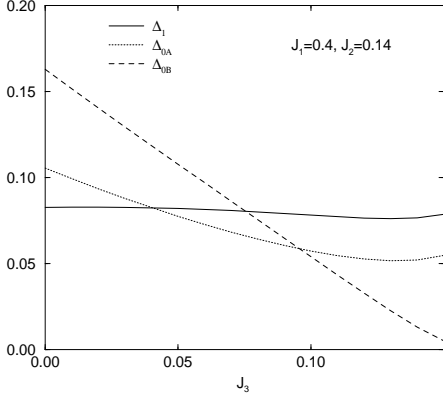


Fig. 3. Excitations Δ_{0A} , Δ_{0B} and Δ_1 .

For simplicity, we fix the 2-N interaction as $J_1 = 0.4$. The gapless 2 phase does not appear in this case. Here, we consider two excitations having $M = L/2$ and $k = \pi$, because the change in the lowest energy level in this sector occurs when J_3 is increased. Then, we define $E_A(L, \frac{L}{2}, \pi)$ ($E_B(L, \frac{L}{2}, \pi)$) as the lower energy in the region of large J_2 (J_3) and small J_3 (J_2), and also define Δ_{0A} (Δ_{0B}) in the same way as the eq. (7). These two excitations $E_A(L, \frac{L}{2}, \pi)$ and $E_B(L, \frac{L}{2}, \pi)$ correspond to the Néel and dimer excitations (see ref. 13) in the picture of the pseudo spin \mathbf{T} , and can be distinguished by the eigenvalues P of the space inversion operation of the rung number $i \rightarrow L - i + 1$. Namely, when $L = 4n$, the state for $E_A(L, \frac{L}{2}, \pi)$ has $P = -1$ and that for $E_B(L, \frac{L}{2}, \pi)$ has $P = +1$. In the spin fluid (gapless 1), plateau A and plateau B phases, the lowest excitations should be Δ_1 , Δ_{0A} and Δ_{0B} , respectively. Therefore, the phase boundaries can be determined from the level crossing points among these three excitations.¹³⁾ Figure 3 shows these three excitations as functions of J_3 when $J_1 = 0.4$, $J_2 = 0.14$, $L = 12$. Thus, the state is gapless for $J_3 < 0.040$, plateau A for $0.040 < J_3 < 0.095$, and plateau B for $J_3 > 0.095$. Repeating such procedures with sweeping the parameters, we obtain the phase diagram of the $J_2 - J_3$ plane as shown in Fig. 4. In order to investigate the universality of the boundary between the gapless and plateau A phases, we estimate the central charge c by¹⁹⁾

$$\frac{1}{L}E\left(L, \frac{L}{2}, 0\right) = \epsilon_\infty - \frac{\pi}{6}c v_s \frac{1}{L^2} \quad (L \rightarrow \infty). \quad (8)$$

where v_s is the sound velocity, which can be calculated by

$$v_s = \frac{L}{2\pi} \left[E\left(L, \frac{L}{2}, \frac{2\pi}{L}\right) - E\left(L, \frac{L}{2}, 0\right) \right], \quad (L \rightarrow \infty) \quad (9)$$

We also estimate the critical exponent η_z defined by $\langle S_0^z S_r^z \rangle - \langle S^z \rangle^2 \sim (-1)^r r^{-\eta_z}$ by use of¹³⁾

$$\eta_z = \frac{L}{2\pi v} (3\Delta_{0A} + \Delta_{0B}) \quad (10)$$

near the gapless 1-plateau A boundary. We note that the

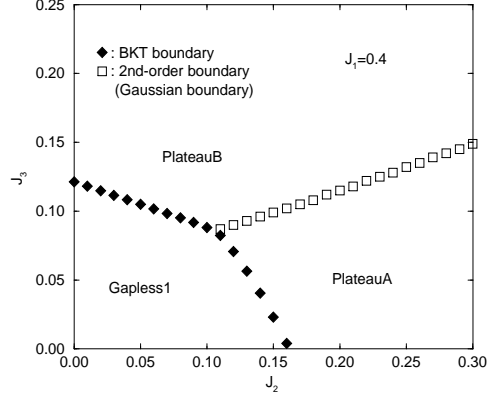


Fig. 4. Phase diagram of the J_2 - J_3 plane with fixed $J_1 (=0.4)$ at $m = 1/2$.

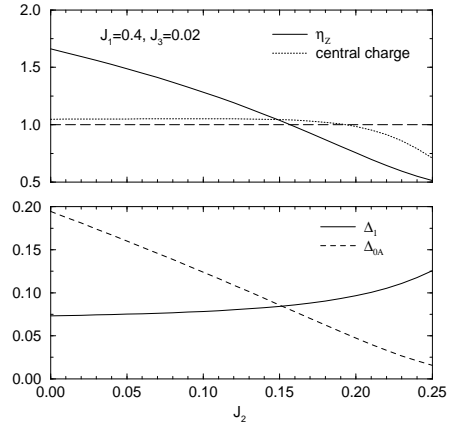


Fig. 5. Central charge c and critical exponent η_z near the BKT boundary between the gapless and plateau A phases, as well as excitations Δ_1 and Δ_{0A} .

roles of Δ_{0A} and Δ_{0B} are interchanged near the gapless 1-plateau B boundary. Since the most dominant logarithmic size corrections are canceled out in eq. (10),¹³⁾ we can obtain an accurate value of η_z from eq. (10). At the BKT transition point of the present type, the exponent η_z should be unity. Figure 5 shows the behaviors of c and η_z near the gapless 1-plateau A boundary, as well as the level cross between Δ_1 and Δ_{0A} , resulting in $J_2^{(cr)} \simeq 0.15$. We can clearly see that $\eta_z \simeq 1$ at $J_2^{(cr)}$, which strongly confirms the universality class of the BKT transition. The behavior of c also suggests the BKT transition. A similar conclusion is also obtained for the gapless 1-plateau B transition.

To clarify the properties of the boundary between plateaux A and B, we show the J_3 dependence of the scaled gap $2L\Delta_1$ ($2\Delta_1$ is the length of the plateau of system size L) along the line $J_2 = 0.3$ in Fig. 4. The size dependence of the scaled gap suggests that the plateau is opening in both phases and that the system is gapless only at the boundary $J_3 \simeq 0.15$. We also found $c = 1$ on the line labeled by open squares in Fig. 4. These results

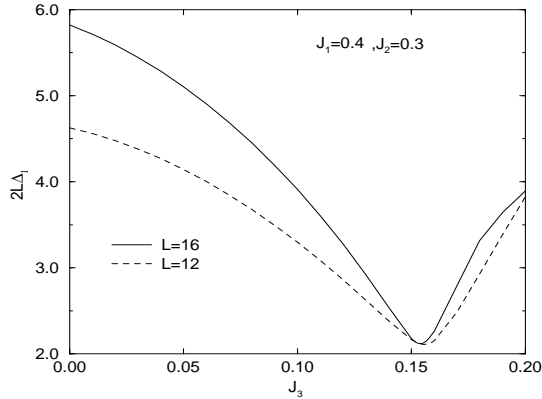


Fig. 6. Behavior of the scaled gap $2L\Delta_1$ in the $J_1=0.4$ and $J_2 = 0.3$ case.

are consistent with the Gaussian fixed line predicted by degenerate perturbation theory.

Several magnetization curves are also presented on line $J_2 = 0.3$; $J_3 = 0, 0.10, 0.15$ and 0.20 . They are obtained by the size scaling analysis²⁰⁾ based on conformal field theory and Shanks transformation²¹⁾, using the numerical result of $E(L, M, k)$ up to $L = 16$. Only the lines of fitting polynomials are shown in Fig. 7. This suggests

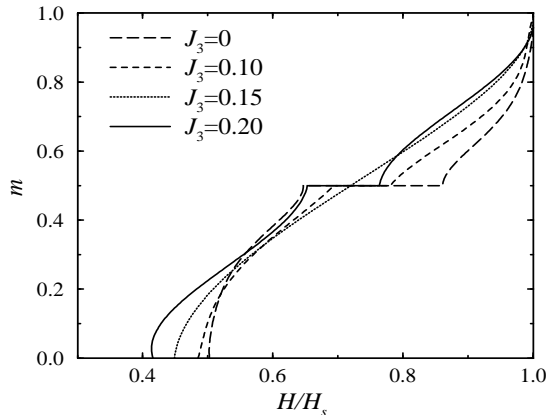


Fig. 7. Magnetization curves for $J_1 = 0.4$ and $J_2=0.3$, with various J_3 ($=0, 0.05, 0.1, 0.15$ and 0.2).

that, with increasing J_3 , the plateau decreases until vanishing at the critical point and then increases again. This behavior also explains why the mechanism of the gap formation due to J_3 is different from the one due to J_2 .

According to the present analysis, the gapless-plateau critical value of J_3 for $J_2 = 0$ is smaller than that of J_2 for $J_3 = 0$, irrespective of J_1 . In addition, the plateau B phase can appear for any ratio of J_1/J_\perp , although the plateau A phase cannot appear for $J_1/J_\perp > 1$. Thus, the J_3 -induced plateau is more realistic than the one due to J_2 . In fact, a typical spin ladder, SrCu_2O_3 ²²⁾, was reported to hold $J_1/J_\perp \sim 2$. Thus, a plateau might be caused by the 3-N coupling of J_3 in this or related materials.

In summary, the magnetization process of the frustrated spin ladder was investigated with degenerate perturbation theory and the level spectroscopy. The present analysis revealed the appearance of a novel magnetization plateau at $m = 1/2$ due to the 3-N interaction. The mechanism of this plateau is explained by the spontaneous dimerization of the pseudo spin system. As far as we know, this is the first theoretical finding of the change in the plateau mechanisms, both of which have the spontaneous symmetry breaking, by sweeping physically natural parameters.

References

- [1] E. Lieb, T. D. Schultz and D. C. Mattis: Ann. Phys. (N. Y.) **16** (1961) 407.
- [2] M. Oshikawa, M. Yamanaka, and I. Affleck: Phys.Rev.Lett. **78** (1997) 1984.
- [3] K. Hida: J. Phys. Soc. Jpn. **60** (1991) 1347 .
- [4] E. Dagotto, J. Riera and D. Scalapino: Phys. Rev. B **45** (1992) 5744.
- [5] M. Troyer, H. Tsunetsugu and T. M. Rice: Phys. Rev. B **53** (1996) 251.
- [6] D. C. Cabra, A. Honecker and P. Pujol: Phys. Rev. Lett. **79** (1997) 5126.
- [7] D. C. Cabra and M. D. Grynberg: Phys.Rev.Lett.**82** (1999) 1768.
- [8] N. Okazaki, J. Miyoshi and T. Sakai: J. Phys. Soc. Jpn. **69** (2000) 37.
- [9] K. Totsuka: Phys.Rev.**B57** (1998) 3435.
- [10] T. Tonegawa, *et al.*: Physica. **B246-247** (1998) 509.
- [11] T. Tonegawa, K. Okamoto and M. Kaburagi: in preparation
- [12] F. Mila: Eur. Phys. J. **B6** (1998) 201.
- [13] K. Nomura and K. Okamoto: J. Phys. A: Math. Gen. **27** (1994) 5773.
- [14] V. L. Berezinski: Zh. Eksp. Teor. Fiz. **59** (1970) 907; Sov. Phys. JETP **32** (1971) 493.
- [15] J. M. Kosterlitz and D. J. Thouless: J.Phys.C **6** (1973) 1181
- [16] K. Okamoto, T. Tonegawa, Y. Takahashi and M. Kaburagi: J. Phys. A: Math. Gen **11** (1999) 10485.
- [17] T. Sakai and N. Okazaki: J. Appl. Phys. to appear.
- [18] K. Okamoto: in preparation.
- [19] J. L. Cardy: J. Phys. A **17** (1984) L385(1984); H.W.Blöte, J. L. Cardy and M. P. Nightingale: Phys. Rev. Lett. **56** (1986) 742; I.Affleck, *ibid.*:**746** (1986).
- [20] T. Sakai and M. Takahashi: Phys.Rev.B **57** (1998) R3201.
- [21] D. Shanks: J. Math. Phys. **34** (1955) 1.
- [22] M. Azuma, *et al.*: Phys. Rev. Lett **73** (1994) 3463.